



Published in final edited form as:

*Nat Commun.* ; 6: 6375. doi:10.1038/ncomms7375.

## Generation of cellular immune memory and B-cell immunity are impaired by natural killer cells

Carolyn Rydyznski<sup>1,2</sup>, Keith A. Daniels<sup>3</sup>, Erik P. Karmele<sup>1</sup>, Taylor R. Brooks<sup>1</sup>, Sarah E. Mahl<sup>1</sup>, Michael T. Moran<sup>1,2</sup>, Caimei Li<sup>1,2</sup>, Rujapak Sutiwisesak<sup>4</sup>, Raymond M. Welsh<sup>3,4</sup>, and Stephen N. Waggoner<sup>1,2</sup>

<sup>1</sup>Center for Autoimmune Genomics and Etiology, 240 Albert Sabin Way, MLC 15012, Cincinnati Children's Hospital Medical Center, Cincinnati, OH, 45229

<sup>2</sup>Immunology Graduate Program, 3333 Burnet Avenue, MLC 7038, Cincinnati Children's Hospital Medical Center, Cincinnati, OH, 45229

<sup>3</sup>Department of Pathology, 368 Plantation Street, ASC9-2014E, University of Massachusetts Medical School, Worcester, MA, 01605

<sup>4</sup>Program in Immunology and Microbiology, 55 Lake Avenue North, University of Massachusetts Medical School, Worcester, MA, 01655

### Abstract

The goal of most vaccines is the induction of long-lived memory T and B cells capable of protecting the host from infection by cytotoxic mechanisms, cytokines and high-affinity antibodies. However, efforts to develop vaccines against major human pathogens like HIV and HCV have not been successful, thereby highlighting the need for novel approaches to circumvent immunoregulatory mechanisms that limit induction of protective immunity. Here we show that mouse natural killer (NK) cells inhibit generation of long-lived virus-specific memory T- and B-cells as well as virus-specific antibody production after acute infection. Mechanistically, NK cells suppressed CD4 T cells and follicular helper T cells (T<sub>FH</sub>) in a perforin-dependent manner during the first few days of infection, resulting in a weaker germinal center (GC) response and diminished immune memory. We anticipate that innovative strategies to relieve NK cell-mediated suppression of immunity should facilitate development of efficacious new vaccines targeting difficult-to-prevent infections.

---

Users may view, print, copy, and download text and data-mine the content in such documents, for the purposes of academic research, subject always to the full Conditions of use:[http://www.nature.com/authors/editorial\\_policies/license.html#terms](http://www.nature.com/authors/editorial_policies/license.html#terms)

Address correspondence and reprint requests to Dr. Stephen N. Waggoner, Center for Autoimmune Genomics and Etiology, Cincinnati Children's Hospital Medical Center, 240 Albert Sabin Way, S9.214, MLC 15012, Cincinnati, OH 45229. Phone 513-803-4607. Fax 513-636-3068. Stephen.Waggoner@cchmc.org.

#### Author contributions

The project was conceived by S.N.W. and R.M.W. Experimental design was determined by C.R., S.N.W., and R.M.W. Acquisition, analysis and interpretation of data was performed by C.R., K.A.D., E.P.K., T.R.B., S.E.M., M.T.M., C.L., R.S. and S.N.W. The manuscript was drafted by S.N.W. and C.R., with critical revisions and intellectual contributions from all of the other authors.

#### Competing financial interests

The authors declare no competing financial interests.

## INTRODUCTION

The development and widespread application of vaccines transformed global health by substantially reducing the threats associated with small pox, measles, polio, and a myriad of other infectious diseases. Nonetheless, infectious pathogens still contribute to a substantial fraction of worldwide mortality owing to the difficulty in developing efficacious vaccines against other microbial threats, including HIV and hepatitis C virus (HCV). While the success of licensed vaccines depends in large part upon the ability of these regimens to mimic the induction of protective immunity that occurs after natural infection<sup>1</sup>, the correlates of immunity and basis for induction of such responses are markedly less apparent with pathogens (e.g. HIV) that cause persistent infection. Moreover, the heightened mutability of HIV and HCV as well as the poor immunogenicity of conserved viral epitopes pose substantial barriers to vaccine-induced immunity<sup>2, 3</sup>. Although the difficulties associated with these viruses as vaccine targets are inescapable, host immunoregulatory factors that limit the generation of protective immune responses may be amenable to interventions aimed at enhancing vaccine efficacy. An improved understanding of host factors that impair the induction of long-lived, protective anti-viral immunity should permit development of new vaccine regimens that circumvent these immunoregulatory mechanisms to engender improved immune responses against challenging vaccine targets.

NK cells are innate immune effector lymphocytes that kill virus-infected cells and thereby represent an important component of antiviral immunity<sup>4</sup>. Recent evidence has highlighted the importance of another property of NK cells, that of contributing to immune defense through regulation of adaptive immunity<sup>5</sup>. Target-cell killing and production of interferon gamma (IFN- $\gamma$ ) by NK cells has been reported to augment isotype class-switching by B cells<sup>6, 7</sup> and to enhance the generation of memory T cell responses<sup>8, 9, 10, 11</sup>. In contrast, NK cells can inhibit adaptive anti-viral immunity during persistent virus infection through production of immunosuppressive cytokines like IL-10<sup>12</sup>, by modulating the function of antigen-presenting cells<sup>13, 14, 15</sup>, or by directly targeting T cells<sup>16, 17, 18</sup>. We recently demonstrated that NK cell-mediated lysis of activated CD4 T cells at an early stage of persistent infection of mice with the clone 13 strain of lymphocytic choriomeningitis virus (LCMV) was critical for prevention of fatal immunopathology<sup>16</sup>. This NK cell-mediated immunoregulation contributed to exhaustion of virus-specific T cells and viral persistence<sup>16, 18, 19</sup>.

Here, we explored the consequences of NK cell-mediated immune regulation on generation of memory T cell responses and the induction of humoral immunity after acute infection of mice. Our results show that NK cells suppress the development of memory T cell responses. In addition, we demonstrate that NK cells inhibit the development of B cell responses resulting in fewer antigen-specific plasma cells and reduced levels of neutralizing antibodies. Together, these findings highlight the potential for NK cell-targeted treatments to improve immune responses in the context of vaccination or infection.

## RESULTS

### Enhanced control of acute infection in absence of NK cells

In the context of persistent LCMV<sup>16, 18, 19</sup>, NK cells have been shown to contribute to viral persistence by indirectly facilitating exhaustion and dysfunction of virus-specific CD8 T cells by lysing activated CD4 T cells<sup>16</sup>. Here, we examined whether NK cells similarly impacted the control of virus replication during acute infection. Intraperitoneal (i.p.) inoculation of C57BL/6 mice with  $5 \times 10^4$  plaque-forming units (p.f.u.) of the Armstrong or clone 13 strains of LCMV results in an acute infection cleared in approximately one week by virus-specific CD8 T cells. As previously shown<sup>20</sup>, NK cell deletion during the first three days of LCMV infection had little effect on LCMV titer. However, beginning at day 4 post-infection, when the T cell response begins to develop, viral titers were better controlled in the spleen during both acute Armstrong (Figure 1A) and clone 13 (Figure 1B) infections when NK cells were depleted (NK) by i.p. administration of 25  $\mu$ g of anti-NK1.1 monoclonal antibody (clone PK136) one day prior to infection. This dose of anti-NK1.1 selectively eliminates bona fide CD3<sup>-</sup>/NK1.1<sup>+</sup> NK cells while leaving NK/T cells intact<sup>16, 21</sup>. Similarly enhanced viral clearance was observed in NK cell-depleted mice during acute infection with  $1.5 \times 10^7$  p.f.u. of Pichinde virus (PICV), a New World arenavirus (Figure 1C).

Since altered viral clearance could impact antigen presentation, we examined the proportion and number of various antigen-presenting cells in the spleens at different times after infection with the Armstrong or clone 13 strains of LCMV (Supplementary Fig. 1). There were few differences between control and NK mice during either infection with regards to the proportion of CD8 $\alpha$ <sup>+</sup> CD11c<sup>+</sup> dendritic cells (DC), PDCA-1<sup>+</sup> B220<sup>+</sup> plasmacytoid DCs (pDC), or F4/80<sup>+</sup> CD11b<sup>+</sup> macrophages (M $\phi$ ) among lineage-negative (CD3<sup>-</sup>CD19<sup>-</sup>NK1.1<sup>-</sup>) cells. However, there were small increases in the number of CD8 $\alpha$ <sup>+</sup> and CD11b<sup>+</sup> DCs at days 4 and 5 after LCMV clone 13 infection, and in the number of pDC at day 5 of Armstrong or day 3 of clone 13 infection. Likewise, there were similar levels of the cytokines IFN- $\gamma$ , tumor necrosis factor (TNF), interleukin-10 (IL-10), IL-6 and IL-2 in the sera of control and NK mice during infection with LCMV Armstrong or clone 13 (Supplementary Fig. 2). Together, this suggests that inflammation and antigen-presenting cell frequencies are relatively similar in the presence and absence of NK cells despite altered levels of replicating virus.

### Depressed antiviral T cell responses in presence of NK cells

Control of acute infections with LCMV and PICV is mediated by virus-specific CD8 T cells, and increased numbers of LCMV- (Figure 1D) and PICV-specific (Figure 1E) IFN- $\gamma$ -expressing CD8 T cells were in the spleens of NK cell-depleted mice relative to NK cell-replete controls at day 6 and 7 of infection, coincident with the diminished virus burden in the absence of NK cells (Figure 1A,C). The phenotype of responding CD8 T cells during acute infection can be a faithful indicator of the propensity of these cells to contract or become memory cells. Specifically, memory precursor effector cells (MPECs) express high levels of the IL-7 receptor alpha chain (IL-7R $\alpha$  or CD127) and low levels of killer cell lectin-like receptor subfamily G member 1 (KLRG1), whereas short-lived effector cells

(SLECs) display the inverse (CD127<sup>-</sup>KLRG1<sup>+</sup>) phenotype<sup>22</sup>. Here, LCMV GP33- and NP396-specific CD8 T cells were identified in the spleen at day 6 of LCMV Armstrong infection by peptide-loaded MHC class I tetramer staining, and then examined for expression levels of KLRG1 and CD127. The proportion and number of MPEC (CD127<sup>+</sup>KLRG1<sup>-</sup>) virus-specific CD8 T cells was increased among GP33 (Figure 1F) and NP396 (Control =  $2.3 \pm 0.38 \times 10^4$  MPEC; NK =  $9.6 \pm 2.0 \times 10^4$  MPEC, n = 8, 2 replicates,  $p = 0.000028$ , Student's *t*-test) tetramer-reactive CD8 T cells in the absence of NK cells. Whereas the number and percentage of SLEC phenotype (CD127<sup>-</sup>KLRG1<sup>+</sup>) GP33-tetramer-reactive CD8 T cells was not changed by NK cell depletion (Figure 1F), there was a reduced proportion (Figure 1F) but increased number (Control =  $6.4 \pm 0.57 \times 10^4$  SLEC; NK =  $17.0 \pm 5.0 \times 10^4$  MPEC, n = 8, 2 replicates,  $p = 0.018$ , Student's *t*-test) of NP396-tetramer reactive CD8 T cells with a SLEC phenotype that likely reflects the increased total number of NP396-specific CD8 T cells (Figure 1D) in the absence of NK cells. Similar results were obtained during acute infection with the clone 13 strain of LCMV (Supplementary Fig. 3A). Thus, NK cells repress the number of virus-specific CD8 T cells and the generation of MPECs during acute virus infection.

### NK cells restrict the generation of memory T-cells

An increase in the magnitude of primary T cell responses during acute infection in the absence of NK cells, as well as the increased frequency of MPEC phenotype cells, could contribute to an enhanced generation of memory T cells after infection of NK cell-depleted mice. In fact, depletion of NK cells prior to an acute course of infection with the clone 13 strain of LCMV resulted in enhanced numbers of memory CD8 (Figure 2A) and CD4 (Figure 2B) T cells 7 weeks later. Moreover, the proportion of memory NP396-specific CD8 (Figure 2C) and GP61-specific CD4 T cells (Figure 2D) capable of simultaneous production of multiple cytokines (left: IFN- $\gamma$ /TNF; right: IFN- $\gamma$ /TNF/IL-2) was increased in mice that had been depleted of NK cells during acute infection. Similar results were observed at 12 weeks after acute infection with the clone 13 strain of LCMV (Supplementary Fig. 3B). The magnitudes of LCMV-specific CD4 (Figure 2E) and CD8 (Supplementary Fig. 3C) memory T cell responses were also enhanced by NK cell depletion during acute infection with the Armstrong strain of LCMV. Likewise, ablation of NK cells during acute LCMV Armstrong infection boosted the proportion of LCMV-specific memory CD8 and CD4 T cells capable of simultaneous production of multiple cytokines (Figure 2F). In a similar fashion, depletion of NK cells prior to acute PICV infection resulted in an enhanced proportion (Figure 3A) and number (Figure 3B) of virus-specific memory CD8 T cells 73 days later. Notably, subdominant responses against the PICV-encoded epitopes NP205 and NP122<sup>23</sup> were markedly enriched. Thus, NK cells can regulate the magnitude, breadth, and the quality of the memory T cell response

A previous study found that NK cells restricted the number of ovalbumin-specific OT-I TCR-transgenic memory CD8 T cells generated after immunization with ovalbumin in lipopolysaccharide and reported that the NK-cell receptor, NKG2D, played an important role in this regulation<sup>24</sup>. However, we had previously demonstrated that NKG2D, which is encoded by the gene *klrk1*, was not required for virus-induced NK cell-mediated lysis of CD4 T cells<sup>16</sup>. Likewise, NKG2D was dispensable in the regulation of virus-specific

memory T-cells described in our current study. The frequency of PICV NP38 tetramer-reactive memory CD8 T cells was comparable in wild-type and NKG2D-deficient mice 54 days after acute PICV infection (Supplementary Fig. 4A). NK-cell depletion augmented memory responses to a similar extent regardless of whether NKG2D was present. Similarly, NK cells repressed the frequency of IFN- $\gamma$ <sup>+</sup> LCMV NP396-specific memory CD8 T cells 49 days after acute infection with  $5 \times 10^4$  p.f.u. of LCMV clone 13 irrespective of the expression of NKG2D (Supplementary Fig. 4B). Thus, NK cell-mediated suppression of virus-specific memory T-cell responses is a general feature of different virus infections and occurs independently of NKG2D.

### NK cells impair T<sub>FH</sub> cell responses

Based on our previous demonstration that virus infection triggers NK-cell lysis of activated CD4 T cells<sup>16</sup>, we hypothesized that NK cells would suppress the development of follicular helper CD4 T cells (T<sub>FH</sub>)<sup>25</sup> and subsequent humoral immune responses. In fact, NK cell-depleted mice harbored a greater proportion of both activated (CD44<sup>hi</sup>CD49d<sup>+</sup>) and T<sub>FH</sub> (CXCR5<sup>+</sup>PD-1<sup>+</sup>) cells among gated CD4<sup>+</sup> T cells compared to control mice at day 6 of LCMV Armstrong infection (Figure 4A, left 3 panels). Notably, the percentage of gated activated (CD44<sup>hi</sup>CD49d<sup>+</sup>) CD4 T cells with a T<sub>FH</sub> phenotype (CXCR5<sup>+</sup>PD-1<sup>+</sup>) was also enhanced in NK cell depleted mice (Figure 4A, far right panel). Thus, the augmented quantity of activated CD4 T cells in the absence of NK cells is comprised of increased numbers of both T<sub>FH</sub> (CXCR5<sup>+</sup>PD-1<sup>+</sup>) and non-T<sub>FH</sub> (CXCR5<sup>-</sup>PD-1<sup>-</sup>) cells (Figure 4B).

Increased proportions of LCMV GP61-specific CD4 T cells were also evident in the spleens of NK cell-depleted mice at day 7 of LCMV Armstrong infection, as determined by MHC class II tetramer staining (Figure 4C, left). Remarkably, the proportion (Figure 4C, middle) and number (Figure 4C, right) of these LCMV-specific CD4 T cells displaying a T<sub>FH</sub> phenotype, here determined by expression of CXCR5 and CD73<sup>26</sup>, was measurably increased in the absence of NK cells. This suggests that the increased T<sub>FH</sub> response in NK cell-depleted mice is not merely a consequence of enhanced T cell activation, but that these T<sub>FH</sub> cells are preferentially expanded as part of a larger augmentation of the virus-specific CD4 T cell response. Expression of inducible T-cell costimulator (ICOS), which is critical for T<sub>FH</sub> functionality<sup>27, 28</sup>, was similar as determined by mean fluorescence intensity (MFI) of staining (Control,  $1145 \pm 176$  ICOS MFI ( $\pm$  denotes s.e.m. throughout text); NK  $1296 \pm 58$  ICOS MFI;  $n = 4$ , 1 of 2 replicates,  $p = 0.15$ , Student's *t*-test) on tetramer-reactive CD4 T cells with a T<sub>FH</sub> phenotype (CXCR5<sup>+</sup>CD73<sup>+</sup>) in control and NK cell-depleted mice. Enhanced numbers of T<sub>FH</sub> cells were also apparent in the spleen 6 days after PICV (Control =  $9.2 \pm 2.9 \times 10^4$  T<sub>FH</sub> cells; AGM1 =  $13.6 \pm 0.53 \times 10^4$  T<sub>FH</sub> cells,  $n = 4$ , 1 of 2 replicates,  $p = 0.050$ , Student's *t*-test) or 7 days after *Listeria monocytogenes* infection (Figure 4D), suggesting that NK-cell inhibition of T<sub>FH</sub> is a general feature of diverse systemic infections.

### NK cell suppression of GC responses

NK cell killing of activated CD4 T cells<sup>16</sup> and suppression of T<sub>FH</sub> responses would likely have profound consequences for CD4 T cell-dependent aspects of humoral immunity, including the formation of germinal centers (GCs). Consistent with this hypothesis, T<sub>FH</sub> and GC B cell (GL7<sup>+</sup>Fas<sup>+</sup>CD19<sup>+</sup>B220<sup>+</sup>) responses were concomitantly enhanced in the spleen

and lymph nodes (LNs) at days 6 to 7 of LCMV Armstrong ( $5 \times 10^4$  p.f.u.) infection (Figure 5A). We also observed an increased proportion and number of GC B cells in NK cell-depleted mice 14 days after infection with LCMV Armstrong (Figure 5B), a time when the GC response is at its peak. Enumeration of the number of peanut agglutinin (PNA)- and anti-B220-reactive GC areas in longitudinal sections of the spleen at day 14 of infection revealed that control and NK cell-depleted spleens appeared to harbor a similar number of these PNA<sup>+</sup>B220<sup>+</sup> structures (Figure 5C), suggesting that NK cells may restrict the cellularity of GCs more so than their frequency during acute infection.

Anti-NK1.1 administration could affect other NK1.1-expressing cells, including NK/T cells. However, our regimen of 25  $\mu$ g of anti-NK1.1 did not deplete NK/T cells<sup>16</sup> and NK cell-depletion enhanced both T<sub>FH</sub> (Supplementary Fig. 5A) and GC B-cell numbers (Supplementary Fig. 5B) at day 8 of Armstrong infection in the LNs of CD1d-deficient (*Cd1d*<sup>-/-</sup>) mice, which are devoid of classical invariant NK/T cells. Moreover, depletion of NK cells in BALB/c mice using a limiting dose of anti-asialo GM1 antibody (AGM1) that eliminates most NK cells while leaving T cell responses intact<sup>29</sup> also enhanced the resulting number of T<sub>FH</sub> cells in the spleen at day 8 after infection with  $5 \times 10^4$  p.f.u. LCMV Armstrong i.p. (Control =  $5.5 \pm 1.5 \times 10^5$  T<sub>FH</sub> cells; AGM1 =  $16.2 \pm 3.0 \times 10^5$  T<sub>FH</sub> cells, n = 3, 1 of 2 replicates,  $p = 0.033$ , Mann Whitney test), and caused an appreciable increase in the number of GC B cells after LCMV Armstrong infection of BALB/c (Figure 5D) and C57BL/6 (data not shown) mice. Increased GC B cell responses were also observed in the spleen 6 days after infection (Control =  $9.4 \pm 3.3 \times 10^4$  GC B cells, NK1.1 =  $19.6 \pm 8.7 \times 10^4$  GC B cells, n = 8, total of 2 replicates,  $p = 0.016$ , Student's *t*-test) with a low dose of LCMV clone 13 ( $5 \times 10^4$  p.f.u. i.p.) and on day 8 after infection (Control =  $5.1 \pm 0.96 \times 10^5$  GC B cells, NK1.1 =  $10.3 \pm 1.2 \times 10^5$  GC B cells, n = 8, total of 2 replicates,  $p = 0.0023$ , Student's *t*-test) with a high intravenous (i.v.) dose of LCMV clone 13 ( $2 \times 10^6$  p.f.u.). Finally, a fraction of the observed GC B cell response could have been a response against bovine serum present in our viral stocks. Thus, we utilized high-titer LCMV Armstrong preparations diluted 400-fold in serum-free Hank's balanced salt solution (iLN 14 d.p.i., Control =  $5.5 \pm 0.59\%$  GC among B cells, NK1.1 =  $9.6 \pm 0.75\%$  GC among B cells, n = 23, 4 replicates,  $p = 0.00005$ , Student's *t*-test) to demonstrate that this phenomenon is independent of bovine serum contamination. Together these results demonstrate that NK-cell suppression of GC reactions is a feature of different types of infections and is not a nuance of C57BL/6 mice or the anti-NK1.1 antibody used to selectively deplete NK cells.

### NK cells limit antibody and long-lived humoral immunity

The GC response primarily functions to facilitate differentiation of B cells into long-lived plasma cells that populate the bone marrow as well as to enable somatic hypermutation of immunoglobulin sequences<sup>30</sup>. When infected with LCMV Armstrong in the absence of NK cells, C57BL/6 mice harbored a modestly increased number of LCMV-specific antibody-secreting cells (ASCs) in the spleen three weeks after infection, as determined by ELISPOT against LCMV-infected and mock-infected BHK lysates (Figure 6A). Importantly, while LCMV-specific ASC were largely absent from the bone marrow of NK cell-sufficient mice at this early time point 21 days post-infection (d.p.i.), there was already a substantial number of these cells present in the bone marrow of NK cell-depleted mice (Figure 6A). Moreover,

the number of long-lived bone marrow ASC, which likely represent plasma cells, was enhanced in mice inoculated with virus in the absence of NK cells relative to NK cell-sufficient control mice 74 to 82 days after infection (Figure 6B). Thus, NK cell suppression of GC responses is associated with reduced frequencies of LCMV-specific ASCs for months after infection.

Somatic hypermutation of immunoglobulin sequences in the GC facilitates affinity maturation and development of high-affinity neutralizing antibodies (nAbs)<sup>30</sup>. Such nAbs usually appear very late (i.e. 3 months) after LCMV infection<sup>31, 32</sup> and are relatively weak in comparison to responses after infections with other viruses, including vesicular stomatitis virus (VSV)<sup>33</sup>. Serum from C57BL/6 mice four weeks after infection with LCMV Armstrong demonstrated little ability to neutralize LCMV (Figure 6C) in a plaque reduction assay<sup>34</sup>, wherein most sera were completely devoid of such activity. A greater proportion of sera from NK cell-depleted Armstrong-infected mice demonstrated a measureable level of neutralizing activity, and although the levels were very low compared to viruses that potently induce nAbs (e.g. VSV)<sup>33</sup>, mean neutralizing activity was slightly elevated in NK cell-depleted mice (Figure 6C). The levels of LCMV-specific nAb (Figure 6D) were also increased in the sera of NK cell-depleted mice relative to control mice at later time points after acute LCMV Armstrong infection. However, there were wide variations in antibody responses within experiments as well as between stocks of virus. Thus, despite a substantial enhancing effect of NK cell depletion on T<sub>FH</sub> and GC B cell responses, statistically significant reductions in virus-specific antibody responses in the presence of NK cells were modest and somewhat variable between experiments.

### B cell-independent suppression of T<sub>FH</sub> by NK cells

Examination of very early time points (day 5 p.i.) of LCMV infection revealed that NK cell depletion resulted in an enhanced number of T<sub>FH</sub> (CXCR5<sup>+</sup>PD-1<sup>+</sup>) cells (Figure 7A) prior to the measureable detection of GC responses at levels that exceed those observed in uninfected mice (Figure 7B). GC B-cell responses were not detectable until day 6 or 7 p.i. in the spleen and other LNs (Figure 5A). Thus, NK cell-mediated suppression of T<sub>FH</sub> responses can be measured at times preceding appearance of GC B cell responses.

To determine whether B cells played a part in NK cell inhibition of T<sub>FH</sub> responses, we infected B cell-deficient ( $\mu$ MT<sup>-/-</sup>)<sup>35</sup> mice with LCMV Armstrong. At day 5 p.i., the percentage and number of NK cells in the spleen was increased in infected control mice relative to their naïve and NK cell-depleted counterparts (Figure 7C). Of greater significance, the proportion and number of T<sub>FH</sub> cells was elevated in the spleen at 5 days p.i. in NK cell-depleted mice relative to non-depleted controls (Figure 7D). Thus, NK cells are capable of impairing T<sub>FH</sub> responses in the absence of an intact B cell compartment.

### Role for CD4 T cells in augmented humoral immunity

To examine the role of CD4 T cells in the NK cell control of the GC B cell response, we depleted CD4 T cell-deficient *cd4*<sup>-/-</sup> mice<sup>36</sup> of NK cells prior to infection with LCMV. As expected for a T-cell-dependent humoral response, LCMV-specific ASC and plasmablast (CD138<sup>+</sup>IgD<sup>-</sup>) B cells were largely undetectable or below levels present in uninfected mice

in the spleens of  $cd4^{-/-}$  mice at day 14 of infection, regardless of the presence or absence of NK cells (Figure 7E). Surprisingly, a weak GC B cell response was measurable in NK cell-depleted  $cd4^{-/-}$  mice but not in NK cell-replete  $cd4^{-/-}$  controls (Figure 7F). Moreover, the number of IgD<sup>-</sup> activated B cells was increased in the absence of NK cells in  $cd4^{-/-}$  mice (Control =  $2.5 \pm 1.7 \times 10^5$  IgD<sup>-</sup> B cells, NK1.1 =  $5.0 \pm 2.2 \times 10^5$  IgD<sup>-</sup> B cells, n = 8, 2 replicates,  $p = 0.023$ , Student's *t*-test). Overall, the weak B cell responses and marginal changes in these responses upon NK cell depletion in CD4 T cell-deficient mice suggests that NK cell suppression of CD4 T cell responses likely plays a more prominent role in the inhibition of humoral immune responses than any direct effects of NK cells upon B cells.

### NK cells act during initial days of acute infection

To determine at what stage of infection NK cell suppression of memory T cell and B cell immune responses takes place, we first examined the duration of NK cell depletion during infection. To our surprise, a single injection of anti-NK1.1 antibody one day before LCMV Armstrong infection maintained an effective depletion of more than 50% of circulating NK cells for 4 weeks (Figure 8A). Therefore, an alternative strategy was needed to evaluate the timing of the NK cell suppressive effect. Towards this end, anti-NK1.1 antibody was administered 3 or 6 days after infection. Two weeks after infection, virus-specific IFN- $\gamma$ -expressing T cell (Figure 8B) and GC B cell (Figure 8C) responses were enhanced in the spleen and LNs, respectively, of mice depleted of NK cells prior to infection (day -1) but not in mice depleted of NK cells at day 3 or 6 after infection. These results suggest that NK cells suppress T and B cell responses at a very early stage of infection (before day 3), consistent with the prior studies by our group<sup>16</sup> and others<sup>19</sup> in the persistent LCMV clone 13 infection model.

### Role for perforin in NK cell suppression of humoral immunity

Cytotoxicity is a major effector function exerted by NK cells in the elimination of virus-infected and transformed target cells. To determine whether cytotoxicity is involved in NK cell regulation of humoral immunity, perforin-deficient mice ( $prf1^{-/-}$ )<sup>37</sup> were depleted of NK cells or treated with isotype control antibody one day prior to infection with LCMV Armstrong. At an early stage of infection prior to the severe pathology associated with lack of viral control and aberrant responses of  $prf1^{-/-}$  CD8 T cells, the proportion (Figure 9A) and number (Figure 9B) of T<sub>FH</sub> cells was measurably enhanced by NK cell depletion in wild-type mice. T<sub>FH</sub> cells were also elevated in  $prf1^{-/-}$  mice regardless of the presence or absence of NK cells. NK cell depletion resulted in enhancement of splenic T<sub>FH</sub> responses in wild-type mice and in *lpr* mice with a dysfunctional Fas/FasL axis<sup>38</sup> (Figure 9C). Therefore, NK cell suppression of humoral immunity is independent of Fas/FasL but requires a perforin-mediated pathway. In support of a role for perforin in NK cell-mediated suppression of the GC response, a marked increase in the spontaneous degranulation of NK cells as determined by *ex vivo* CD107a/b staining<sup>39</sup> was observed in the spleen and lymph nodes following infection with LCMV (Figure 9D). While the nature of the NK cell cytotoxicity receptors potentially involved in this NK cell-mediated immunoregulation are unclear, we did observe that NKG2D was similarly dispensable for NK cell-mediated suppression of T<sub>FH</sub> and GC B cells (Supplementary Fig. 4C) and virus-specific T-cell memory responses after acute infection (Supplementary Fig. 4A,B).



## Discussion

These results demonstrate that NK cells inhibit the induction of humoral immunity and memory T cells following an array of acute infections. Notably, NK cells contributed to delayed and diminished GC reactions that were subsequently associated with decreased LCMV-specific antibody and plasma cell responses. Moreover, the quantity and quality of T-cell memory was reduced by NK-cell activities during acute infection. Consideration of these suppressive functions of NK cells in the context of vaccination could unveil innovative means of enhancing humoral and cellular responses against vaccine-associated antigens.

The enhancement of LCMV-specific ASC and antibody responses in mice that had been transiently depleted of NK cells during acute infection represents a compelling new way to think about the contribution of innate responses to the development of protective humoral immunity. Increased generation of bone marrow plasma cells (i.e. ASCs) and improved elaboration of nAbs in the absence of NK cells indicates that there are measureable consequences of NK cell suppression of the GC response, including restriction of somatic hypermutation and affinity maturation of virus-specific antibody<sup>30</sup>. Yet, despite the profound effects of NK cell depletion on T<sub>FH</sub> and GC B cell responses, differences in neutralizing antibody formation were modest in most experiments and sometimes not statistically significant. An explanation may be that the curtailed antigen levels after NK cell depletion of acutely infected mice, likely resulting from the enhanced CD8 T cell responses (Figure 1), are insufficient to efficiently promote the expansion of the B cell response and affinity maturation of antibodies. The consistent two-fold increase in the number of bone marrow ASCs coupled with the more marginal and sporadic gains in nAb titers could reflect the delicate balance between the need for B cells in the germinal center to undergo repeated rounds of somatic hypermutation versus the propensity of these cells to undergo terminal differentiation into long-lived plasma cells<sup>30</sup>, which no longer mutate their antigen receptor. In future studies, it will be of great interest to examine the molecular changes in these GC B cells in the presence and absence of NK cells in order to evaluate expression of *Blimp1/Prdm1*<sup>40</sup>, which determines plasma cell differentiation, as well as to examine the extent of somatic hypermutation of immunoglobulin sequences in these cells. Moreover, it will be important to determine if NK cells influence the development of vaccine-induced nAbs against clinically relevant pathogens, like HIV.

Examination of the underlying factors contributing to enhanced humoral immune responses in the absence of NK cells showed that in the absence of CD4 T cells, plasmablasts and LCMV-specific ASC were largely absent in the spleen of LCMV infected mice and that the accelerated appearance of differentiated T<sub>FH</sub> cells in NK cell-deficient mice preceded the development of GC B cell responses. These findings suggest that the suppressive effect of NK cells on B-cell responses is a consequence of NK cell-mediated inhibition of T<sub>FH</sub> responses. In fact, we confirmed that B cells are not required for CD4 T cells to differentiate into T<sub>FH</sub> cells, and that NK cell-mediated suppression of T<sub>FH</sub> responses occurs even in the absence of B cells. Nevertheless, plasmablast responses were trending higher in NK cell-depleted *cd4*<sup>-/-</sup> mice while activated IgD<sup>low</sup> and GC B cell responses were enhanced by NK cell depletion in the absence of CD4 T cells. This could reflect an additional effect of NK cells, beyond the suppression of T<sub>FH</sub> responses, that is either mediated directly upon B cells

or via regulation of other leukocytes (i.e. NK/T cells, basophils or CD8 T cells)<sup>41, 42, 43</sup> capable of providing B cell help.

Following LCMV infection, NK cells in the spleen and lymph nodes displayed increased levels of the degranulation markers CD107a and CD107b compared to uninfected mice, suggesting that NK cells within these tissues of infected mice are cytotoxic. The loss of granule-mediated cytotoxicity in perforin-deficient mice resulted in an increased number of T<sub>FH</sub> cells after LCMV infection that was similar to levels observed in NK cell depleted perforin-sufficient wild-type mice. Moreover, NK cell depletion failed to further enhance the T<sub>FH</sub> response in perforin-deficient mice. In contrast, Fas-deficient *lpr* mice were readily amenable to NK cell-depletion mediated enhancement of T<sub>FH</sub> responses, suggesting that the Fas/FasL system is dispensable in this NK cell-mediated suppression. These results are consistent with our previous finding that NK cells can lyse CD4 T cells<sup>16</sup>, and point to a prominent role for perforin-mediated cytolysis in NK cell suppression of humoral immunity. Nevertheless, we have not ruled out a direct perforin-dependent effect of NK cells on B cells. B cells, however, may be protected from the direct cytolytic effects of NK cells because B cells express high levels of CD48<sup>44</sup>, which delivers negative signals to murine NK cells<sup>45</sup>.

It remains unclear whether the NK cell-mediated control of T<sub>FH</sub> cells is due to a direct effect of NK cells upon differentiated T<sub>FH</sub> cells or a result of a diminished number of activated CD4 T cells capable of differentiating into T<sub>FH</sub> cells. There was an increased proportion of activated CD4 T cells with a T<sub>FH</sub> phenotype, suggesting that these cells are preferentially inhibited. However, there were increased numbers of both T<sub>FH</sub> and non-T<sub>FH</sub> CD4 T cells in NK cell-depleted mice, indicating that the suppression exerted by NK cells may be more broadly applied to multiple lineages of differentiated CD4 T cells. Notably, the suppressive activity of NK cells upon both T and B cell responses was primarily mediated during the initial three days of infection, which may indicate that NK cells interfere with an early step in the activation and differentiation of CD4 T cells. Future studies will also aid in determining whether NK cells influence T cell activation and T<sub>FH</sub> differentiation via direct effects on CD4 T cells, as we previously described in a chronic infection model<sup>16</sup>, or through inhibition of antigen-presenting cell function<sup>13, 19, 46, 47</sup>.

The simplest explanation for increased numbers of memory T cells lies in the substantially elevated magnitude of primary T cell responses during acute infection. If a constant fraction of cells is lost during contraction, this larger pool of effector T cells should directly translate to a greater quantity of memory T cells. However, memory cell differentiation is not a stochastic process, but has instead been linked to the expression of the IL-2 (CD25) and IL-7 (CD127) receptor alpha chains on activated T cells with enhanced potential to develop into long-lived memory cells<sup>48, 49</sup>. As early as 2 or 3 days post-infection, precursors of memory T cells can be distinguished based on low expression of the IL-2 receptor alpha chain<sup>48, 50</sup>. Notably, this early fate determination of virus-specific T cells coincides with the peak of NK cell-mediated suppression of virus-specific T cells observed during the first 3 days of LCMV clone 13 infection<sup>16, 19</sup>. Therefore, diminished antiviral memory T cell responses after infection in the presence of NK cells may be a consequence of NK cell-mediated elimination of precursors of these memory T cells at very early stages of the response. In

fact, analysis of tetramer-reactive LCMV-specific CD8 T cells at an early stage of infection demonstrated that NK cells are associated with a reduced fraction and number of T cells with a memory precursor (CD127<sup>+</sup> KLRG1<sup>-</sup>) phenotype. Thus, NK cells may restrict memory T cell development by limiting the differentiation of memory precursor cells.

It is important to note that NK cells can also exert beneficial effects on T and B cell responses during vaccination. Notably, NK cell-derived IFN- $\gamma$  can promote antigen-presenting cell functionality, T<sub>H</sub>1 differentiation of T cells, and isotype-class switching in B cells. Moreover, immunization of mice with apoptotic splenocytes expressing membrane-bound ovalbumin (OVA) resulted in development of memory OVA-specific CD8 T cell responses that were enhanced by the presence of NK cells during priming<sup>8</sup>. In contrast, immunization of mice with OVA protein admixed with bacterial lipopolysaccharide resulted in impaired generation of OVA-specific memory CD8 T cell as a consequence of NK cell-mediated suppression<sup>24</sup>. We speculate that inflammation associated with virus infection triggers NK cell-mediated suppression of memory T cell development, such that the occurrence of this inhibition may vary widely depending on the nature of the vaccine regimen (i.e. live virus versus protein subunit) or the adjuvant (i.e. alum versus CpG DNA) used. Therefore, careful selection of adjuvants to optimize the beneficial effects of inflammation on memory T cell development while minimizing interference by NK cells represents one viable approach to enhancing vaccine efficacy.

In addition, further studies aimed at determining whether NK cells similarly suppress memory T and B cells will reveal whether NK cell-mediated immunoregulation can have compound effects upon prime-boost vaccination strategies or during re-vaccination of immune individuals.

## Methods

### Mice

C57BL/6, BALB/c, *cd4*<sup>-/-</sup>,  *$\mu$ MT*<sup>-/-</sup>, *prf1*<sup>-/-</sup>, and *lpr* mice were purchased from The Jackson Laboratories (Bar Harbor, ME). *Klrk1*<sup>-/-51</sup> on a C57BL/6 background were obtained from Bojan Polic (University of Rijeka). C57BL/6 *cd1d*<sup>-/-</sup> were obtained from Mark Exley<sup>52</sup> (University of Manchester) or David Hildeman<sup>53</sup> (CCHMC), respectively. Male mice at 6–12 weeks of age (at onset of infection) were routinely utilized in experiments. Mice were housed under pathogen-free conditions, and experiments were performed using ethical guidelines approved by the Institutional Animal Use and Care Committees of the University of Massachusetts Medical School and Cincinnati Children's Hospital Medical Center. In many experiments, randomization was achieved by randomly assigning mice within a cage to different experimental groups or by modulating the processing order of the mice at time of harvest.

### *In vivo* NK Cell Depletion

One day before infection, selective depletion<sup>16</sup> of NK cells was attained through a single intraperitoneal (i.p.) injection of 25  $\mu$ g/mouse anti-NK1.1 monoclonal antibody (PK136) or 25  $\mu$ g/mouse of a control mouse IgG2a (C1.18.4) produced by Bio-X-Cell (West Lebanon,

NH). Alternatively, NK Cells were depleted through a single i.p. injection with 20  $\mu$ L of anti-asialo GM1 (Wako Biochemicals, Richmond, VA) diluted in 180  $\mu$ L of Hank's balanced salt solution (HBSS) or 20  $\mu$ L of normal rabbit serum (Wako Pure Chemical Industries, Japan) diluted in 180  $\mu$ L HBSS.

## Infections

The Armstrong and clone 13 strains of LCMV were propagated in baby hamster kidney cells (BHK21)<sup>54</sup>. Virus was titrated by plaque assay on Vero cells from American Type Culture Collection (ATCC, Manassas, VA). Mice were inoculated with  $5 \times 10^4$  plaque-forming units (p.f.u.) of LCMV Armstrong i.p. The clone 13 strain of LCMV was administered at a dose of  $5 \times 10^4$  i.p. or  $2 \times 10^6$  p.f.u. i.v. PICV was prepared in BHK21 cells and titrated by plaque assay on Vero cells<sup>55</sup>. PICV was administered i.p. at a dose of  $1.5 \times 10^7$  p.f.u./mouse. *L. monocytogenes* (strain 10403S) was grown in brain heart infusion (BHI) medium at 37°C to early log-phase (OD<sub>600</sub> 0.1), washed, suspended in PBS, and inoculated i.v. at a dose of  $3 \times 10^5$  colony-forming units<sup>56</sup>.

## Peptides and tetramers

Synthetic peptides (90% purity by reverse phase-HPLC) representing LCMV-encoded epitopes recognized by T cells in the context of MHC were purchased from 21<sup>st</sup> Century Biochemicals. These peptides include the I<sup>A</sup><sup>b</sup>-presented LCMV GP61-80 or GP64-80 epitope (GLKGPDIYKGVYQFKSVEFD); D<sup>b</sup>-presented LCMV GP33-41 (KAVYNFATC), LCMV GP276-286 (SGVENPGGYCL), LCMV NP396-404 (FQPQNGQFI), and PICV NP122-132 (VYEGNLTNTQL); and the K<sup>b</sup>-presented LCMV NP205-212 (YTVKYPNL), LCMV GP118-125 (ISHNFCNL), PICV NP205-212 (YTVKFPNM), and PICV NP38-45 (SALDFHKV). Production of PICV NP38-45-loaded MHC class I tetramers was previously described<sup>57</sup>. LCMV GP33-41 (KAVYNFATC) and NP396 (FQPQNGQFI) loaded H-2D<sup>b</sup> tetramers were produced at the NIH Tetramer Facility. Class I tetramer staining was performed at room temperature for 45 minutes before addition of surface antibodies. LCMV GP61-80 epitope loaded I-A<sup>b</sup> tetramers were acquired from David Hildeman (CCHMC), and class II tetramer staining was performed at 37°C for 75 minutes prior to surface staining with fluorescent antibodies.

## Antibodies and FACS analysis

Fluorescently-labeled antibodies purchased from BD Biosciences (San Diego, CA) include the following: CD95/Fas (Jo2, 1:200), GL7 (1:200), CD44 (IM7, 1:200), CD4 (RM4-5, 1:400), IL-2 (JES6-5H4, 1:100), NK1.1 (PK136, 1:200), CD45R/B220 (RA3-6B2, 1:200), and CD3 $\epsilon$  (500A2, 1:300). Antibodies purchased from eBioscience (San Diego, CA) include: GL7 (1:200), and PD-1 (RMPI-30, 1:200). Antibodies purchased from BioLegend (San Diego, CA) include: CD8 $\alpha$  (53-6.7, 1:200), CD8 $\beta$  (53-5.8, 1:400), IgD (11-26c.2a, 1:200), CD19 (6D5, 1:200), NK1.1 (PK136, 1:200), NKp46 (29A1.4, 1:50), TNF $\alpha$  (MP6-XT22, 1:200), CXCR5 (L138D7, 1:50), CD45R/B220 (RA3-6B2, 1:200), FR4 (12A5, 1:200), CD73 (TY/11.8, 1:200), F4/80 (BM8, 1:200), CD49d (R1-2, 1:200), ICOS (C398.4A, 1:200), CD11b (M1/70, 1:200), CD138 (281-2, 1:200), CD127 (A7R34, 1:200), KLRG1 (2F1/KLRG1, 1:200), CD107a (1D4B, 1:200), CD107b (M3/84, 1:200), and CD4

(GK1.5, 1:400). Antibodies purchased from Tonbo Biosciences include: CD44 (IM7, 1:200), IFN $\gamma$  (XMG1.2, 1:1,000), CD3 $\epsilon$  (145-2C11, 1:300), CD19 (1D3, 1:200), B220 (RA3-6B2, 1:200), CD11c (N418, 1:200), and CD16/32 (2.4G2, 1:200). Antibodies purchased from Miltenyi Biotec include: CD49b/DX5 (DX5, 1:200) and CD8 $\alpha$  (53-6.7, 1:200). Cells were collected on a LSR II or LSR Fortessa cytometer equipped with FACSDiva software (BD Biosciences), and data were analyzed with FlowJo software (Tree Star, Ashland, OR).

### Lymphocyte preparation and intracellular cytokine assay

Single-cell leukocyte suspensions were prepared from spleens and lymph nodes by mechanical homogenization of tissues between glass slides. Single-cell suspensions from various tissues were plated at  $2 \times 10^6$  cells per well in 96-well plates and either immediately subjected to flow staining or first stimulated for 5 hours at 37°C with 1  $\mu$ M viral peptide in the presence of brefeldin A and 0.2 U mL<sup>-1</sup> recombinant human IL-2. Cells were then incubated with a 1:200 dilution of anti-CD16/32 (Fc block 2.4G2) in flow cytometry buffer (HBSS + 5% FCS) and stained for 20 minutes at 4°C with various combinations of fluorescently-tagged antibodies. Alternatively, cells were first stained at 4°C with tetramers for 40 minutes prior to the 20 minute surface stain. Following staining, cells were washed and permeabilized with BD Cytofix/Cytoperm solution and then stained in BD Perm/Wash using antibodies specific for various intracellular cytokines.

### Antibody-secreting cell (ASC) assay

Multiscreen HA filter ELISPOT plates (EMD Millipore) were coated with 100  $\mu$ L of LCMV-Armstrong infected BHK cell lysates or mock-infected BHK cell lysates at 4° overnight. Plates were UV- irradiated for 10 minutes and the supernatant was aspirated. Plates were washed once with phosphate buffered saline (PBS) containing 0.1% Tween-20 (PBST) and twice with PBS, then blocked with 100  $\mu$ L of media for 3 hours at room temperature. While plates were blocking, bone marrow cells and splenocytes from infected mice were harvested and serially diluted 3-fold in serum-free RPMI-1640 media. After 3 hours, media was aspirated from the plate and 100  $\mu$ L of bone marrow or spleen cells were added to each well and incubated with antigen for 4–5 hours at 37° C. After incubation, the plate was washed 3 times with PBS and 3 times with PBST. A 100  $\mu$ L volume of PBST with 1% FBS and a 1:1,000 dilution of biotin anti-mouse IgG (Life Technologies) was added to each well and incubated overnight at 4°C. The plate was washed 4 times with PBST prior to addition of 100  $\mu$ L of PBST with 1% FBS and a 1:1,000 dilution of streptavidin-HRP (Life Technologies) to each well. The plate was incubated at room temperature for one hour, washed 3 times with PBST and 3 times with PBS, then 100  $\mu$ L of AEC substrate (Life Technologies) was added to each well. The plate was incubated at room temperature for 5 minutes and wells were washed with tap water. Plate was air-dried and spots were counted manually with a dissecting microscope.

### PNA staining of GC reactions

Tissues from mice were placed into 10% buffered formalin. Slides were prepared and stained in the CCHMC Pathology Core. GCs were enumerated by immunohistochemistry (IHC) using anti-B220 antibody (1:50, BD Biosciences) and anti-peanut agglutinin (PNA;

Vector Labs 1:50). All imaging was performed using an Aperio digital slide scanner at 20x magnification, and images were analyzed using ImageScope software (Leica Biosystems).

### Luminex analysis of cytokine expression

IFN- $\gamma$ , TNF $\alpha$ , IL-2, IL-6, IL-10, IL-21 cytokine concentrations in serum supernatants were determined in the Cincinnati Children's Hospital Medical Center Research Flow Cytometry Core by Alyssa Sproles using enzyme-linked immunosorbent assay (ELISA) using Milliplex™ Multiplex kits (Millipore, Billerica, MA) according to manufacturer's protocol. Briefly, in a 96 well black plate, 25  $\mu$ L of sample in duplicate was incubated with 25  $\mu$ L antibody-coated beads overnight at 4°C on a plate shaker. Plates were then washed twice on a vacuum apparatus and 25  $\mu$ L of secondary antibody was added and incubated at room temperature for 1 hour while shaking. Finally, 25  $\mu$ L of streptavidin-RPE was added directly to the secondary antibody and incubated for 30 minutes at room temperature with shaking. Plates were then washed twice and 100  $\mu$ L of sheath fluid was added. Plates were shaken for 5 minutes and then read using luminex technology on the Bio-Plex™ (Bio-Rad, Hercules, CA). Concentrations were calculated from standard curves using recombinant proteins.

### Degranulation assay

Single cell suspensions were kept warm and quickly prepared from spleen and lymph nodes of uninfected C57BL/6 mice or from mice three days after infection with LCMV. Cells were plated at  $2 \times 10^6$  cells per well in 96-well plates and were stimulated for 4 hours at 37°C with brefeldin A (0.2  $\mu$ L mL<sup>-1</sup>) and a 1:200 dilution of FITC conjugated CD107a (1D4B) and CD107b (M3/84) for a total volume of 200  $\mu$ l per well. Following incubation, cells were washed and stained for various other surface markers.

### Plaque reduction (nAb) assay

Neutralizing activity of LCMV-specific antibodies present in sera was measured using a plaque reduction assay<sup>34</sup>. Briefly, heat-inactivated serum was subjected to serial 2-fold dilutions. Then 100  $\mu$ L of diluted serum was incubated with 100  $\mu$ L of defined quantities of LCMV Armstrong for 1.5 hours at 37°C. The amount of infectious virus remaining was measured by standard plaque assay on Vero cells. Results are reported as the log<sub>2</sub> of the greatest dilution able to mediate a 50% reduction in plaque counts.

### Statistical analysis

Experimental results are consistently presented as mean  $\pm$  s.e.m. Statistical differences between control and NK cell-depleted groups were determined using a Mann-Whitney test or the two-tailed unpaired Student's *t*-test depending on whether data demonstrated Gaussian distribution and equal variance. With both tests, a *p* value of < 0.05 was considered significant. Graphing and statistical analyses were performed using either Microsoft Excel or GraphPad Prism (San Diego, CA). In occasional instances, researchers performing the analysis were blinded to the experimental groupings of the animals or serum samples. We estimated the sample size considering the variation and mean of the distribution.

## Supplementary Material

Refer to Web version on PubMed Central for supplementary material.

## Acknowledgments

We thank S. Lazaro for administrative support and A. Sproles for performing Luminex analysis. We thank V. Rathinam, K. Kuang, D. Peppas, E. Szomolanyi-Tsuda, R. Mishra, H. Xu, and F. Raval for technical assistance. We thank D. Hildeman for providing LCMV and class II tetramer, and S. Way for providing *L. monocytogenes*. We acknowledge the NIH Tetramer Core Facility (contract HHSN272201300006C) for provision of MHC tetramers. We thank the CCHMC Pathology Core (supported by NIH grant DK078392) for performing the immunohistochemical assays for GC enumeration. All flow cytometric data were acquired using equipment maintained by the CCHMC Research Flow Cytometry Core, which is supported in part by NIH grants AR47363, DK78392 and DK90971. This work was supported by NIH grants AI007349 and DA038017, a New Scholar Award from The Ellison Medical Foundation, and start-up funds from the Cincinnati Children's Research Foundation (S.N.W.); as well as NIH research grants AI017672, AI109858, and AI046629 (R.M.W.). The views expressed are those of the authors and do not necessarily express the views of the NIH.

## References

1. Plotkin SA. Correlates of protection induced by vaccination. *Clinical and vaccine immunology*. 2010; 17:1055–1065. [PubMed: 20463105]
2. Swadling L, Klenerman P, Barnes E. Ever closer to a prophylactic vaccine for HCV. Expert opinion on biological therapy. 2013; 13:1109–1124. [PubMed: 23651228]
3. Kwong PD, Mascola JR, Nabel GJ. The changing face of HIV vaccine research. *Journal of the International AIDS Society*. 2012; 15:17407. [PubMed: 22789610]
4. Lanier LL. Evolutionary struggles between NK cells and viruses. *Nat Rev Immunol*. 2008; 8:259–268. [PubMed: 18340344]
5. Welsh RM, Waggoner SN. NK cells controlling virus-specific T cells: Rheostats for acute vs. persistent infections. *Virology*. 2013; 435:37–45. [PubMed: 23217614]
6. Michael A, Hackett JJ, Bennett M, Kumar V, Yuan D. Regulation of B lymphocytes by natural killer cells. Role of IFN-gamma. *J Immunol*. 1989; 142:1095–1101. [PubMed: 2492576]
7. Wilder JA, Koh CY, Yuan D. The role of NK cells during in vivo antigen-specific antibody responses. *J Immunol*. 1996; 156:146–152. [PubMed: 8598455]
8. Krebs P, et al. NK-cell-mediated killing of target cells triggers robust antigen-specific T-cell-mediated and humoral responses. *Blood*. 2009; 113:6593–6602. [PubMed: 19406986]
9. Kelly JM, et al. Induction of tumor-specific T cell memory by NK cell-mediated tumor rejection. *Nat Immunol*. 2002; 3:83–90. [PubMed: 11743585]
10. Westwood JA, Kelly JM, Tanner JE, Kershaw MH, Smyth MJ, Hayakawa Y. Cutting edge: novel priming of tumor-specific immunity by NKG2D-triggered NK cell-mediated tumor rejection and Th1-independent CD4+ T cell pathway. *J Immunol*. 2004; 172:757–761. [PubMed: 14707044]
11. Robbins SH, et al. Natural killer cells promote early CD8 T cell responses against cytomegalovirus. *PLoS Pathog*. 2007; 3:e123. [PubMed: 17722980]
12. Lee SH, Kim KS, Fodil-Cornu N, Vidal SM, Biron CA. Activating receptors promote NK cell expansion for maintenance, IL-10 production, and CD8 T cell regulation during viral infection. *J Exp Med*. 2009; 206:2235–2251. [PubMed: 19720840]
13. Andrews DM, et al. Innate immunity defines the capacity of antiviral T cells to limit persistent infection. *J Exp Med*. 2010; 207:1333–1343. [PubMed: 20513749]
14. Mitrovic M, et al. The NK Cell Response to Mouse Cytomegalovirus Infection Affects the Level and Kinetics of the Early CD8+ T-Cell Response. *J Virol*. 2012; 86:2165–2175. [PubMed: 22156533]
15. Stadnisky MD, Xie X, Coats ER, Bullock TN, Brown MG. Self MHC class I-licensed NK cells enhance adaptive CD8 T-cell viral immunity. *Blood*. 2011; 117:5133–5141. [PubMed: 21436069]
16. Waggoner SN, Cornberg M, Selin LK, Welsh RM. Natural killer cells act as rheostats modulating antiviral T cells. *Nature*. 2012; 481:394–398. [PubMed: 22101430]

17. Peppas D, et al. Up-regulation of a death receptor renders antiviral T cells susceptible to NK cell-mediated deletion. *J Exp Med*. 2013; 210:99–114. [PubMed: 23254287]
18. Lang PA, et al. Natural killer cell activation enhances immune pathology and promotes chronic infection by limiting CD8+ T-cell immunity. *Proc Natl Acad Sci U S A*. 2012; 109:1210–1215. [PubMed: 22167808]
19. Cook KD, Whitmire JK. The depletion of NK cells prevents T cell exhaustion to efficiently control disseminating virus infection. *J Immunol*. 2013; 190:641–649. [PubMed: 23241878]
20. Bukowski JF, Woda BA, Habu S, Okumura K, Welsh RM. Natural killer cell depletion enhances virus synthesis and virus-induced hepatitis in vivo. *J Immunol*. 1983; 131:1531–1538. [PubMed: 6309965]
21. Waggoner SN, Taniguchi RT, Mathew PA, Kumar V, Welsh RM. Absence of mouse 2B4 promotes NK cell-mediated killing of activated CD8+ T cells, leading to prolonged viral persistence and altered pathogenesis. *J Clin Invest*. 2010; 120:1925–1938. [PubMed: 20440077]
22. Joshi NS, et al. Inflammation directs memory precursor and short-lived effector CD8(+) T cell fates via the graded expression of T-bet transcription factor. *Immunity*. 2007; 27:281–295. [PubMed: 17723218]
23. Brehm MA, Pinto AK, Daniels KA, Schneck JP, Welsh RM, Selin LK. T cell immunodominance and maintenance of memory regulated by unexpectedly cross-reactive pathogens. *Nat Immunol*. 2002; 3:627–634. [PubMed: 12055626]
24. Soderquest K, et al. Cutting edge: CD8+ T cell priming in the absence of NK cells leads to enhanced memory responses. *J Immunol*. 2011; 186:3304–3308. [PubMed: 21307295]
25. Crotty S. Follicular helper CD4 T cells (TFH). *Annu Rev Immunol*. 2011; 29:621–663. [PubMed: 21314428]
26. Iyer SS, et al. Identification of novel markers for mouse CD4(+) T follicular helper cells. *Eur J Immunol*. 2013; 43:3219–3232. [PubMed: 24030473]
27. Dong C, et al. ICOS co-stimulatory receptor is essential for T-cell activation and function. *Nature*. 2001; 409:97–101. [PubMed: 11343121]
28. McAdam AJ, et al. ICOS is critical for CD40-mediated antibody class switching. *Nature*. 2001; 409:102–105. [PubMed: 11343122]
29. Yang H, Yogeewaran G, Bukowski JF, Welsh RM. Expression of asialo GM1 and other antigens and glycolipids on natural killer cells and spleen leukocytes in virus-infected mice. *Natural immunity and cell growth regulation*. 1985; 4:21–39. [PubMed: 3875791]
30. Victora GD, Nussenzweig MC. Germinal centers. *Annu Rev Immunol*. 2012; 30:429–457. [PubMed: 22224772]
31. Bruns M, Cihak J, Muller G, Lehmann-Grube F. Lymphocytic choriomeningitis virus. VI. Isolation of a glycoprotein mediating neutralization. *Virology*. 1983; 130:247–251. [PubMed: 6636539]
32. Hangartner L, Zinkernagel RM, Hengartner H. Antiviral antibody responses: the two extremes of a wide spectrum. *Nat Rev Immunol*. 2006; 6:231–243. [PubMed: 16498452]
33. Pinschewer DD, et al. Kinetics of protective antibodies are determined by the viral surface antigen. *J Clin Invest*. 2004; 114:988–993. [PubMed: 15467838]
34. Battegay M, Cooper S, Althage A, Banziger J, Hengartner H, Zinkernagel RM. Quantification of lymphocytic choriomeningitis virus with an immunological focus assay in 24- or 96-well plates. *J Virol Methods*. 1991; 33:191–198. [PubMed: 1939506]
35. Kitamura D, Roes J, Kuhn R, Rajewsky K. A B cell-deficient mouse by targeted disruption of the membrane exon of the immunoglobulin mu chain gene. *Nature*. 1991; 350:423–426. [PubMed: 1901381]
36. Rahemtulla A, et al. Normal development and function of CD8+ cells but markedly decreased helper cell activity in mice lacking CD4. *Nature*. 1991; 353:180–184. [PubMed: 1832488]
37. Kagi D, et al. Cytotoxicity mediated by T cells and natural killer cells is greatly impaired in perforin-deficient mice. *Nature*. 1994; 369:31–37. [PubMed: 8164737]
38. Watanabe-Fukunaga R, Brannan CI, Copeland NG, Jenkins NA, Nagata S. Lymphoproliferation disorder in mice explained by defects in Fas antigen that mediates apoptosis. *Nature*. 1992; 356:314–317. [PubMed: 1372394]



39. Alter G, Malenfant JM, Altfeld M. CD107a as a functional marker for the identification of natural killer cell activity. *Journal of immunological methods*. 2004; 294:15–22. [PubMed: 15604012]
40. Herberman RB, Nunn ME, Lavrin DH. Natural cytotoxic reactivity of mouse lymphoid cells against syngeneic acid allogeneic tumors. I. Distribution of reactivity and specificity. *International journal of cancer Journal international du cancer*. 1975; 16:216–229. [PubMed: 50294]
41. Denzel A, et al. Basophils enhance immunological memory responses. *Nat Immunol*. 2008; 9:733–742. [PubMed: 18516038]
42. Maggi E, et al. Th2-like CD8+ T cells showing B cell helper function and reduced cytolytic activity in human immunodeficiency virus type 1 infection. *J Exp Med*. 1994; 180:489–495. [PubMed: 8046328]
43. Galli G, et al. CD1d-restricted help to B cells by human invariant natural killer T lymphocytes. *J Exp Med*. 2003; 197:1051–1057. [PubMed: 12695492]
44. Yokoyama S, Staunton D, Fisher R, Amiot M, Fortin JJ, Thorley-Lawson DA. Expression of the Blast-1 activation/adhesion molecule and its identification as CD48. *J Immunol*. 1991; 146:2192–2200. [PubMed: 1848579]
45. Lee KM, et al. 2B4 acts as a non-major histocompatibility complex binding inhibitory receptor on mouse natural killer cells. *J Exp Med*. 2004; 199:1245–1254. [PubMed: 15123744]
46. Wilson JL, Heffler LC, Charo J, Scheynius A, Bejarano MT, Ljunggren HG. Targeting of human dendritic cells by autologous NK cells. *J Immunol*. 1999; 163:6365–6370. [PubMed: 10586025]
47. Hayakawa Y, et al. NK cell TRAIL eliminates immature dendritic cells in vivo and limits dendritic cell vaccination efficacy. *J Immunol*. 2004; 172:123–129. [PubMed: 14688317]
48. Kalia V, Sarkar S, Subramaniam S, Haining WN, Smith KA, Ahmed R. Prolonged interleukin-2 $\alpha$  expression on virus-specific CD8+ T cells favors terminal-effector differentiation in vivo. *Immunity*. 2010; 32:91–103. [PubMed: 20096608]
49. Kaech SM, Tan JT, Wherry EJ, Konieczny BT, Surh CD, Ahmed R. Selective expression of the interleukin 7 receptor identifies effector CD8 T cells that give rise to long-lived memory cells. *Nat Immunol*. 2003; 4:1191–1198. [PubMed: 14625547]
50. Arsenio J, Kakaradov B, Metz PJ, Kim SH, Yeo GW, Chang JT. Early specification of CD8 T lymphocyte fates during adaptive immunity revealed by single-cell gene-expression analyses. *Nat Immunol*. 2014
51. Zafirova B, et al. Altered NK cell development and enhanced NK cell-mediated resistance to mouse cytomegalovirus in NKG2D-deficient mice. *Immunity*. 2009; 31:270–282. [PubMed: 19631564]
52. Huber S, Sartini D, Exley M. Role of CD1d in coxsackievirus B3-induced myocarditis. *J Immunol*. 2003; 170:3147–3153. [PubMed: 12626572]
53. Mendiratta SK, Martin WD, Hong S, Boesteanu A, Joyce S, Van Kaer L. CD1d1 mutant mice are deficient in natural T cells that promptly produce IL-4. *Immunity*. 1997; 6:469–477. [PubMed: 9133426]
54. Welsh RM, Seedhom MO. Lymphocytic choriomeningitis virus (LCMV): propagation, quantitation, and storage. *Curr Protoc Microbiol*. 2008; Chapter 15(Unit 15A):11.
55. Selin LK, Nahill SR, Welsh RM. Cross-reactivities in memory cytotoxic T lymphocyte recognition of heterologous viruses. *J Exp Med*. 1994; 179:1933–1943. [PubMed: 8195718]
56. Rowe JH, Ertelt JM, Xin L, Way SS. *Listeria monocytogenes* cytoplasmic entry induces fetal wastage by disrupting maternal Foxp3+ regulatory T cell-sustained fetal tolerance. *PLoS Pathog*. 2012; 8:e1002873. [PubMed: 22916020]
57. Shen ZT, et al. Bi-specific MHC heterodimers for characterization of cross-reactive T cells. *J Biol Chem*. 2010; 285:33144–33153. [PubMed: 20729210]

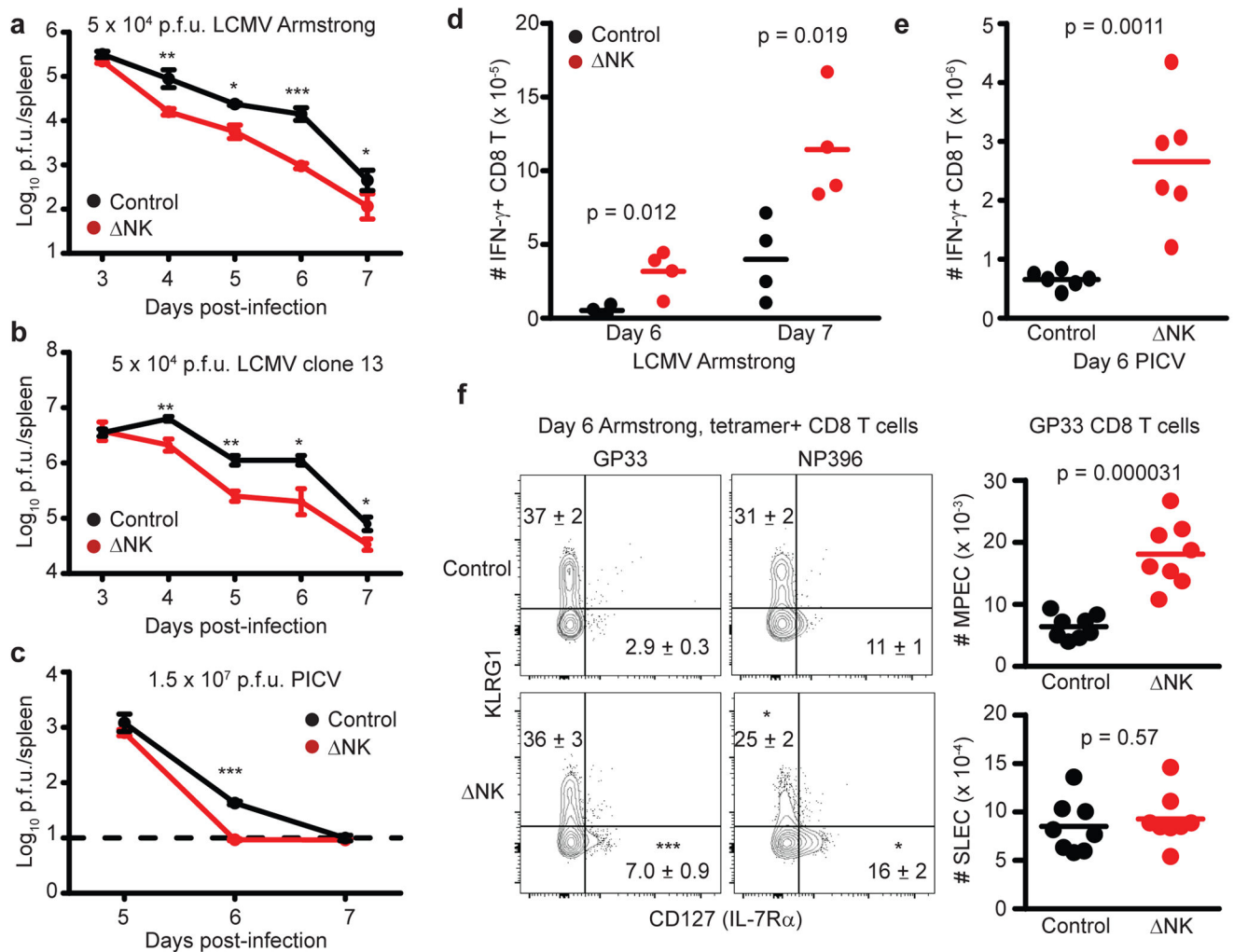


### Figure 1. NK cells limit T cell-mediated antiviral immunity during acute infection

C57BL/6 mice ( $n = 8$  per group) were either treated i.p. with 25  $\mu\text{g}$  NK cell-depleting anti-NK1.1 antibody ( $\Delta\text{NK}$ ) or a non-depleting isotype control (Control) one day before i.p. infection with (a,d,f)  $5 \times 10^4$  p.f.u. of LCMV Armstrong, (b)  $5 \times 10^4$  p.f.u. of LCMV clone 13, or (c,e)  $1.5 \times 10^7$  p.f.u. of PICV ( $n = 3-4$  per group). Statistical differences between groups were determined by Student's  $t$ -test and are denoted as \* $p < 0.05$ , \*\* $p < 0.01$ , \*\*\* $p < 0.001$ , or labeled  $p$  value. (a-c) Viral titers in the spleen ( $\pm$  s.e.m.) were determined at various time points p.i., where dotted line denotes limit of detection. (D,E) At days 6 or 7 after (d) LCMV Armstrong ( $n = 4$ ) or (e) day 6 of PICV infection ( $n = 6$ ), the quantities of IFN- $\gamma$ -expressing (d) LCMV NP396-specific or (e) PICV NP38-specific CD44<sup>hi</sup> CD8 T cells were determined in the spleen by intracellular cytokine staining after *in vitro* restimulation with virus-derived peptides. (f) On day 6 of LCMV Armstrong infection ( $n = 8$ ), virus-specific CD8 T cells were determined by staining with LCMV GP33- or NP396-loaded MHC class I tetramers. FACS plots display expression of KLRG1 and CD127 by gated CD8<sup>+</sup> CD44<sup>hi</sup> tetramer-reactive CD8 T cells with mean ( $\pm$  s.e.m.) proportion (in FACS plots) and number (graphs) of SLEC (KLRG1<sup>+</sup> CD127<sup>-</sup>) and MPEC (KLRG1<sup>-</sup>

CD127<sup>+</sup>) phenotype cells among tetramer-reactive CD8 T cells. All data are representative of two to three independent experiments.

Author Manuscript

Author Manuscript

Author Manuscript

Author Manuscript

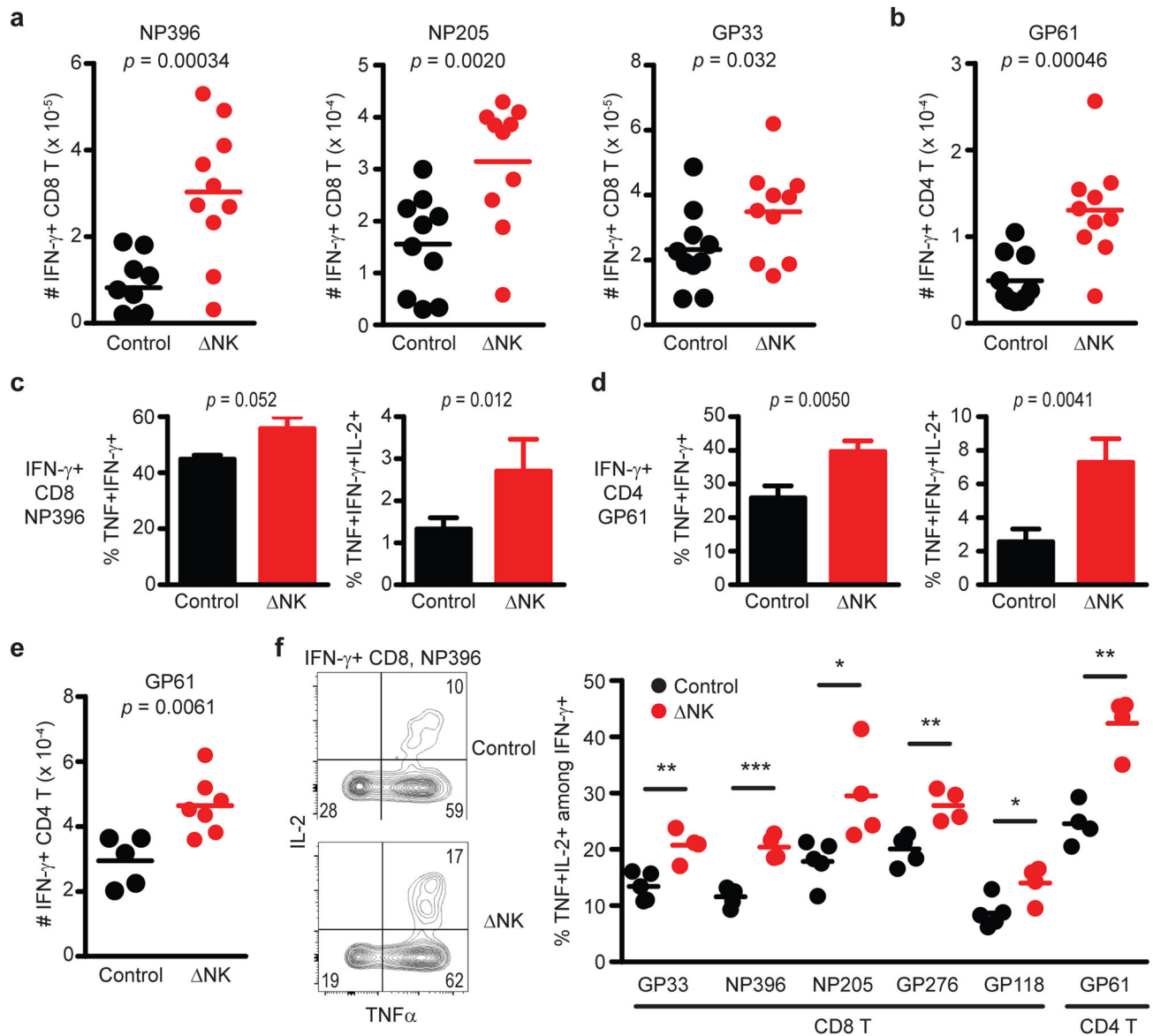


**Figure 2. Magnitude and quality of antiviral memory T cell responses are impaired by NK cells** C57BL/6 mice ( $n = 9$ – $10$  per group) were either treated i.p. with  $25 \mu\text{g}$  anti-NK1.1 antibody (  $\Delta$ NK) or isotype control (Control) one day before i.p. infection with  $5 \times 10^4$  p.f.u. of (a-d) LCMV clone 13 or (e,f) LCMV Armstrong. (a,b) The numbers of splenic IFN- $\gamma$ <sup>+</sup> LCMV-specific (a) CD8 and (b) CD4 T cells were determined 49–52 days p.i. by intracellular cytokine staining after *in vitro* restimulation with virus-derived peptides. The fraction of IFN- $\gamma$ <sup>+</sup> LCMV (c) NP396-specific CD8 and (d) GP61-specific CD4 T cells ( $\pm$  s.e.m.) co-expressing TNF- $\alpha$  (left) or TNF- $\alpha$  and IL-2 (right) is graphed ( $n = 10$  per group). (e) The number of IFN- $\gamma$ <sup>+</sup> GP61-specific CD4 T cells was determined in the spleen 36 days after infection with LCMV Armstrong. (f) The fraction of IFN- $\gamma$ <sup>+</sup> CD8 and CD4 T cells co-expressing TNF- $\alpha$  and IL-2 at day 202 of LCMV Armstrong infection is graphed for mice ( $n = 4$ – $5$  per group) treated with isotype (Control) or anti-NK1.1 antibody (  $\Delta$ NK) one day

before infection. Significant differences between groups were determined by Student's *t*-test and are displayed as \* $p < 0.05$ , \*\* $p < 0.01$ , \*\*\* $p < 0.001$ , or actual *p* value. Data in (a-d) are pooled from two independent experiments, while (e,f) are representative of two similar experiments.

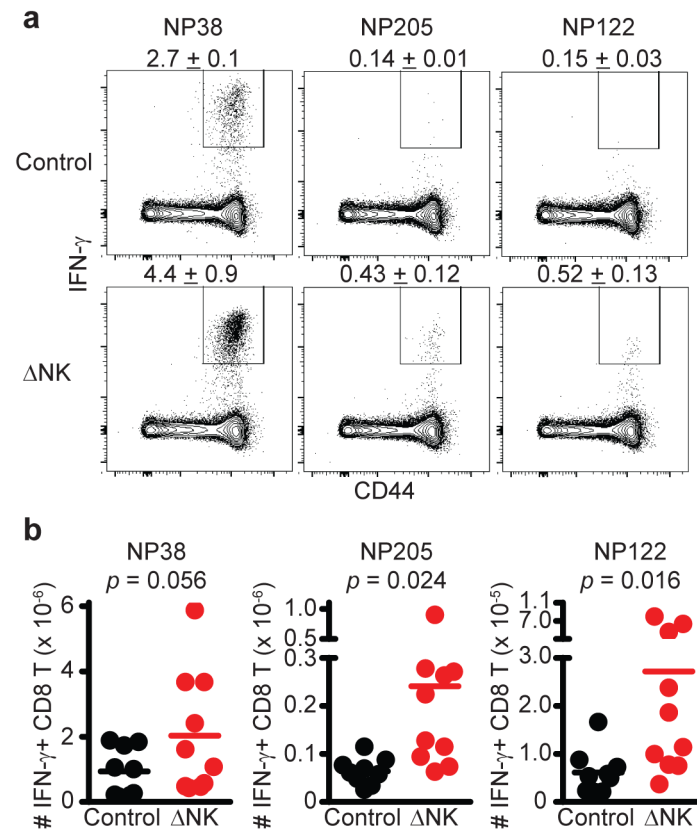


**Figure 3. Greater magnitude and breadth of memory CD8 T cell responses when primed in absence of NK cells**

Following selective depletion of NK cells (ΔNK) or treatment with control antibody (Control), C57BL/6 mice were infected with  $1.5 \times 10^7$  p.f.u. of PICV i.p. At day 73 p.i., the (a) proportion (mean ± s.e.m., n = 5 per group) and (b) number (n = 9–10 per group) of IFN-γ-expressing PICV-specific CD8 T cells was determined in the spleen by intracellular cytokine staining after *in vitro* restimulation with virus-derived peptides. Data in (a) are representative of two independent experiments, while data from two experiments are pooled in (b). Statistical differences between groups were determined by Student's *t*-test.

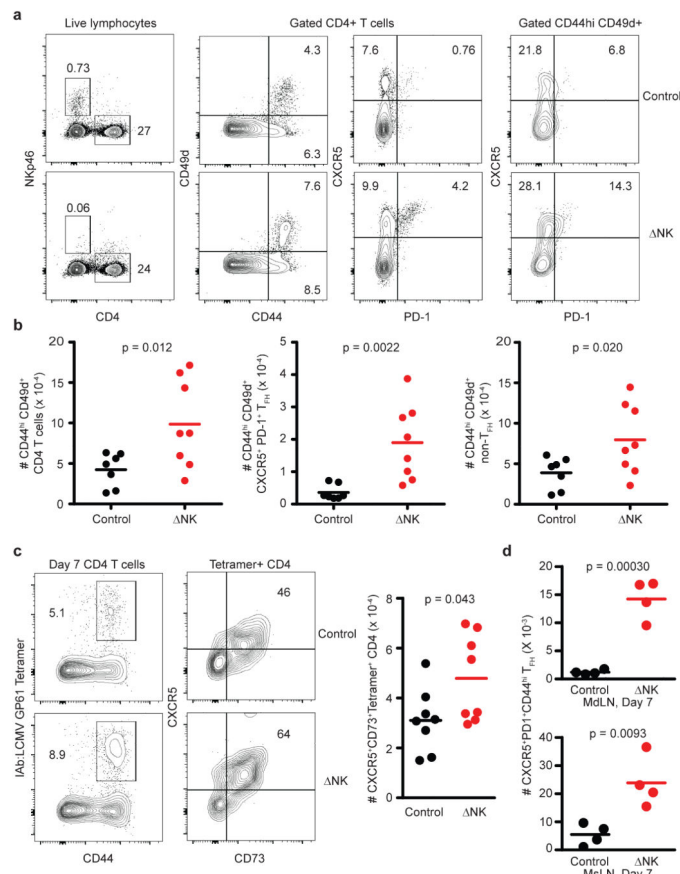


#### Figure 4. NK cells suppress T<sub>FH</sub> responses during infection

Groups of C57BL/6 mice were infected with  $5 \times 10^4$  p.f.u. (i.p.) of (a-c) LCMV Armstrong ( $n = 7-8$  per group) or (d)  $3 \times 10^5$  c.f.u. (i.p.) of *L. monocytogenes* ( $n = 4$  per group) one day after treatment with anti-NK1.1 (NK) or isotype control (Control). (a,b) At day 6 p.i., live singlet lymphocytes in the inguinal LN (left panel, a) were determined to be NK cells (NKp46<sup>+</sup>CD4<sup>-</sup>) or CD4 T cells (NKp46<sup>-</sup>CD4<sup>+</sup>). Gated CD4 T cells (middle panels, b) were analyzed for activation markers CD44 and CD49d or T<sub>FH</sub> markers PD-1 and CXCR5. Activated (CD44<sup>hi</sup>CD49d<sup>+</sup>) CD4 T cells (right panel, a) were further analyzed for expression of PD-1 and CXCR5. Representative FACS plots and proportions are shown in (a), while total numbers of activated (left panel, b: CD44<sup>hi</sup>CD49d<sup>+</sup>), T<sub>FH</sub> (middle panel, b: CD44<sup>hi</sup>CD49d<sup>+</sup> CXCR5<sup>+</sup>PD-1<sup>+</sup>), and non-T<sub>FH</sub> (right panel, b: CD44<sup>hi</sup>CD49d<sup>+</sup> CXCR5<sup>-</sup>PD-1<sup>-</sup>) splenic CD4 T cells for individual mice are shown in (b). (c) At day 7 of infection, splenic CD4 T cells (left panel) were stained with anti-CD44 and LCMV GP61-loaded MHC class II tetramers to determine LCMV-specific CD4 T cells. These cells were examined for markers of T<sub>FH</sub> phenotype CD73 and CXCR5 (middle panel). The total number of LCMV GP61-specific T<sub>FH</sub> cells (CD73<sup>+</sup>CXCR5<sup>+</sup>CD44<sup>hi</sup>Tetramer<sup>+</sup>) in 8 individual mice per group is plotted in right panel. (d) Number of T<sub>FH</sub> (CD44<sup>hi</sup>CD49d<sup>+</sup>CXCR5<sup>+</sup>PD-1<sup>+</sup>) in the mediastinal (MdLN) and mesenteric (MsLN) LNs at day 7 of *L. monocytogenes* infection. Data are pooled from two

independent experiments, and statistically significant differences were determined by Student's *t*-test.

Author Manuscript

Author Manuscript

Author Manuscript

Author Manuscript



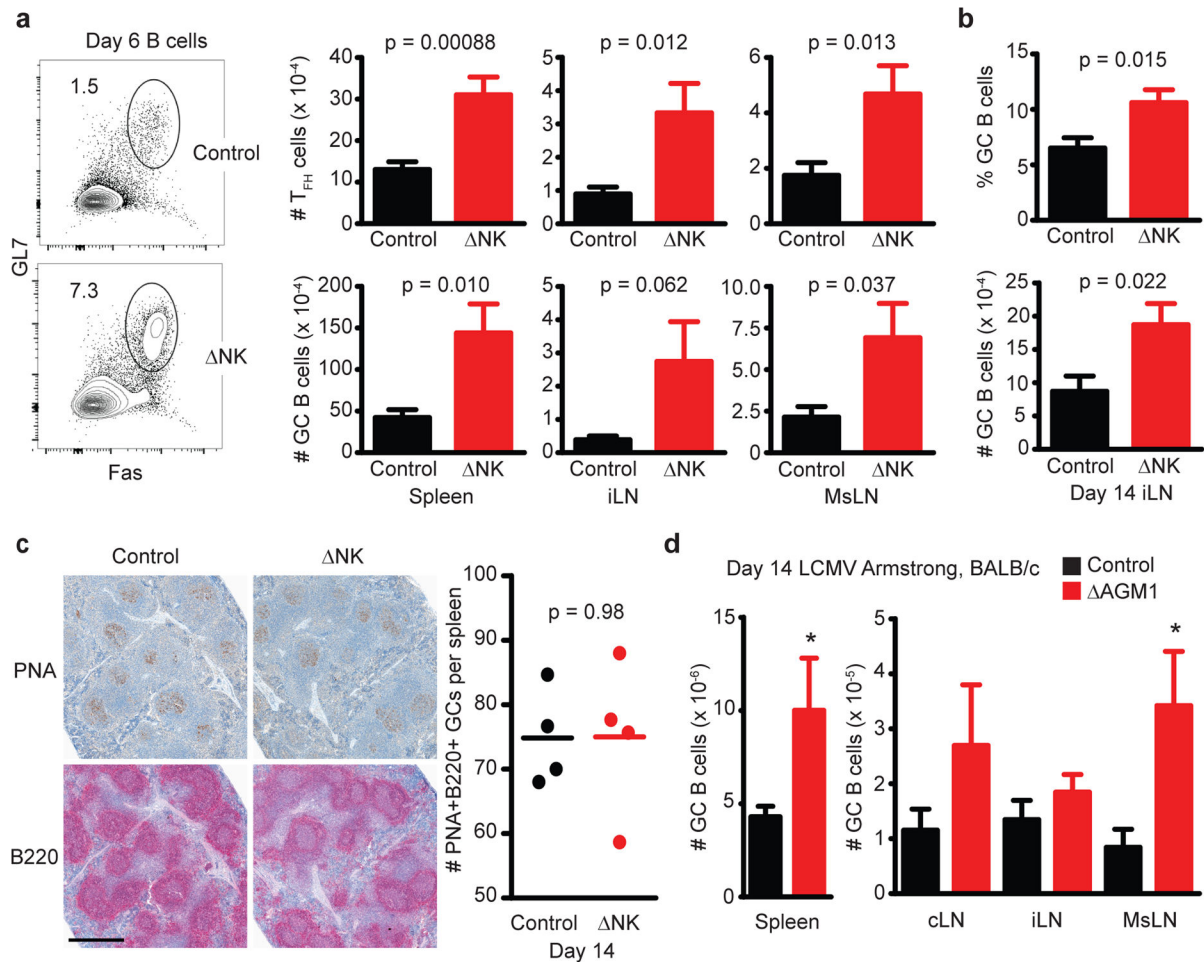


### Figure 5. NK cells suppress germinal center responses after acute virus infection

(a–c) C57BL/6 mice were depleted of NK cells with anti-NK1.1 or administered an equivalent amount of isotype control antibody (Control) one day prior to infection with  $5 \times 10^4$  p.f.u. LCMV Armstrong i.p. (a) Six to seven days p.i., the proportions and numbers of GC (Fas<sup>+</sup>GL7<sup>+</sup>) B cells (B220<sup>+</sup>CD19<sup>+</sup>) and T<sub>FH</sub> cells ( $\pm$  s.e.m.) were determined in the spleen ( $n = 12$  per group), inguinal (iLN;  $n = 12$ –16 per group) nodes, and mesenteric (MsLN;  $n = 12$ –16 per group) nodes. (b) The fraction and number of T<sub>FH</sub> cells in the iLN at day 14 of infection ( $n = 8$  per group). (c) PNA and anti-B220 staining of GC reactions in formalin-fixed spleen sections at day 14 of infection (scale bar = 500 microns). PNA<sup>+</sup>B220<sup>+</sup> GC areas were enumerated in a complete spleen section from 4 mice per group. (d) The frequency of GC B cells in the spleen and lymph nodes at day 14 of LCMV Armstrong ( $5 \times 10^4$  p.f.u. i.p.) infection in groups of BALB/c mice ( $n = 8$  per group) that received normal rabbit serum (control) or 20  $\mu$ L anti-asialoGM1 ( $\Delta$ AGM1) one day prior to infection. All results are representative of two similar experiments. Significant differences between control and NK cell-depleted groups are displayed as  $*p < 0.05$  or given  $p$  value, as determined by Student's  $t$ -test.

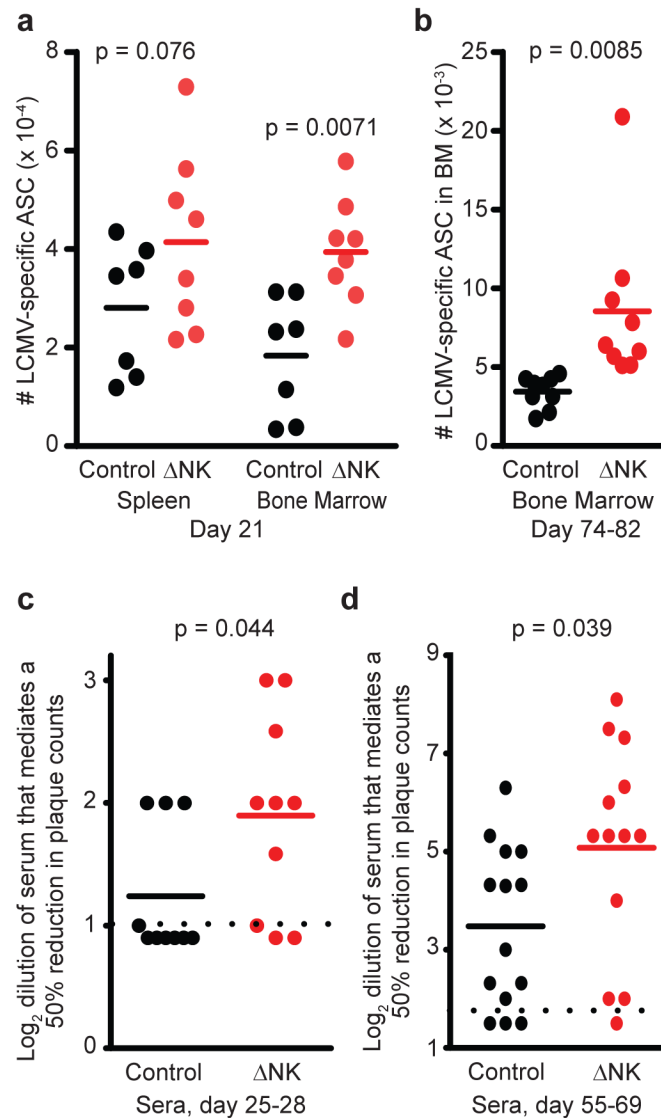


**Figure 6. Enhanced LCMV-specific antibody responses in absence of NK cells**

C57BL/6 mice ( $n = 7-9$  per group) were depleted of NK cells ( $\Delta$  NK) or treated with isotype antibody (control) one day prior to i.p. infection with  $5 \times 10^4$  p.f.u. LCMV Armstrong. (a) 21 or (b) 74 – 82 days p.i., spleen and bone marrow cells were collected and subjected to ELISPOT analysis of antibody-secreting cell (ASC) frequencies. (c) Sera from mice ( $n = 10$  per group) at day 28 p.i. was analyzed for the ability to neutralize LCMV in a plaque-reduction assay, which is graphed as  $\log_2$  of the greatest dilution that could mediate a 50% reduction in plaque-forming units. (d) Neutralizing antibody titers were also determined as in (c) for sera from mice ( $n = 13-14$  per group) 55 – 69 days after LCMV Armstrong infection. Dotted lines represent limit of detection. Data are pooled from 2 to 3 independent experiments, and statistical significance of differences determined by Student's  $t$ -test.

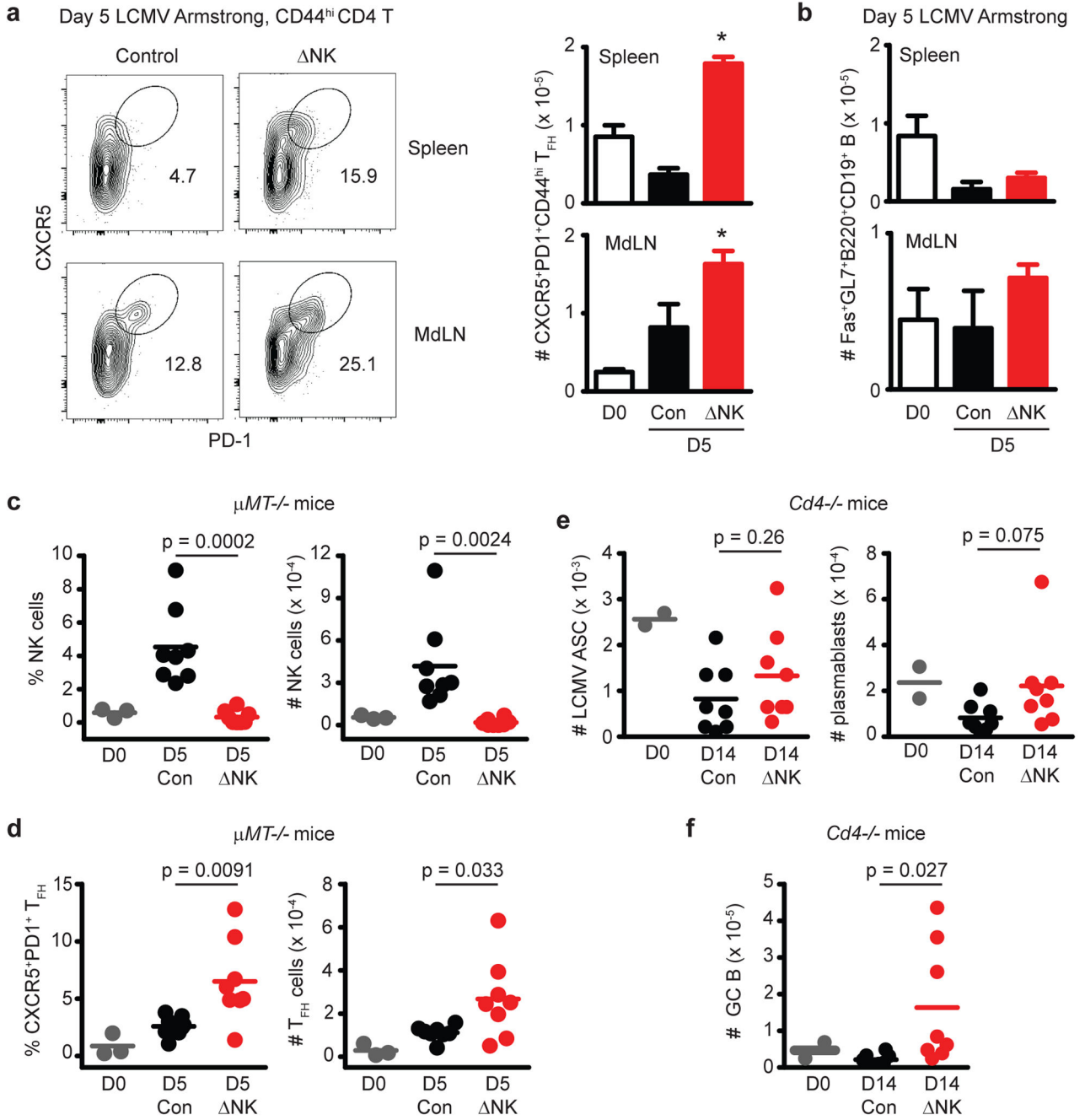


**Figure 7. Inhibition of humoral immunity by NK cells involves CD4 T cells**

C57BL/6 mice were depleted of NK cells (ΔNK) or treated with isotype antibody (Control, Con) one day prior to i.p. infection with  $5 \times 10^4$  p.f.u. of LCMV Armstrong. Significant differences between control and NK cell-depleted groups were determined by Student's *t*-test and are displayed as \**p*<0.05 or actual *p* value. On day 5 after Armstrong infection, frequencies of (a) T<sub>FH</sub> (CXCR5<sup>+</sup>PD1<sup>+</sup>CD44<sup>hi</sup>CD4<sup>+</sup>) cells and (b) GC B (Fas<sup>+</sup>GL7<sup>+</sup>B220<sup>+</sup>CD19<sup>+</sup>) B cells ( $\pm$  s.e.m.) were determined (n = 4 per group) in the spleen and mediastinal LN (MdLN). Results are representative of two similar experiments. (c,d)

$\mu$ MT<sup>-/-</sup> mice (n = 3 for naïve; n = 8 per group for infected) were depleted of NK cells (NK) or treated with control antibody (Con) one day prior to infection with  $5 \times 10^4$  p.f.u. (i.p.) LCMV Armstrong, or left uninfected (D0). The proportion (left) and number (right) of (c) NKp46<sup>+</sup>CD3<sup>-</sup> NK cells or (d) CD44<sup>hi</sup>CXCR5<sup>+</sup>PD1<sup>+</sup> CD4 T cells was determined in the spleen day 5 of infection. (e,f) *Cd4*<sup>-/-</sup> mice were depleted of NK cells (NK) or treated with control antibody (Con) one day prior to infection with  $5 \times 10^4$  p.f.u. (i.p.) LCMV Armstrong (n = 2 for naïve; n = 8 per group for infected). (e) The numbers of plasmablast cells (CD138<sup>+</sup>IgD<sup>-</sup>CD19<sup>+</sup>B220<sup>+</sup>), LCMV-specific antibody-secreting cells, and (f) GC (Fas<sup>+</sup>IgD<sup>-</sup>CD19<sup>+</sup>B220<sup>+</sup>) B cells were determined in the spleen at day 14 of infection. All results are pooled from two independent experiments.

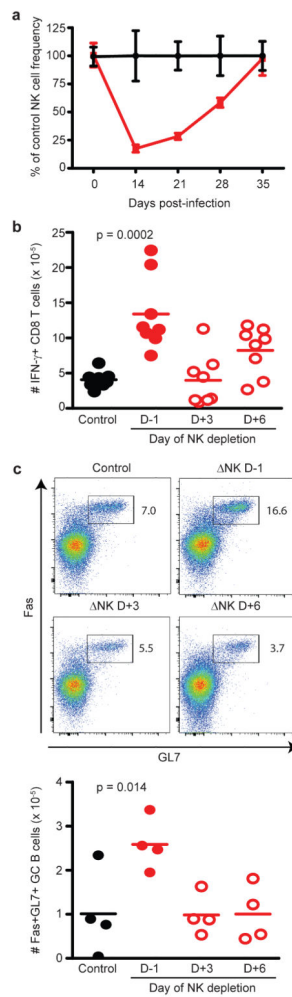


**Figure 8. NK cell suppression of humoral and cellular immunity occurs at early stage of infection** Prior to infection (D-1) with  $5 \times 10^4$  p.f.u. (i.p.) of the Armstrong strain of LCMV, C57BL/6 mice ( $n = 4$  per group) were treated with  $25 \mu\text{g}$  of anti-NK1.1 (NK) or isotype (control) antibody. (a) The frequencies of NK cells ( $\pm$  s.e.m.) were determined in peripheral blood at various times post-infection, and are plotted as a fraction of non-depleted control mice at each time point. (b,c) Additional groups of mice were administered a single dose of anti-NK1.1 depleting antibody at later time points (day 3 (D+3) or day 6 (D+6) p.i.). (b) LCMV-specific CD8 T cell responses in the spleen ( $n = 8$  per group) were measured by intracellular cytokine staining at day 14 p.i. after *in vitro* restimulation with virus-derived peptides. (c) Numbers of GC B cells ( $n = 4$  per group) were determined in the iLN at day 14 p.i. Results are pooled from two independent experiments, and statistically significant differences were determined by Student's *t*-test.

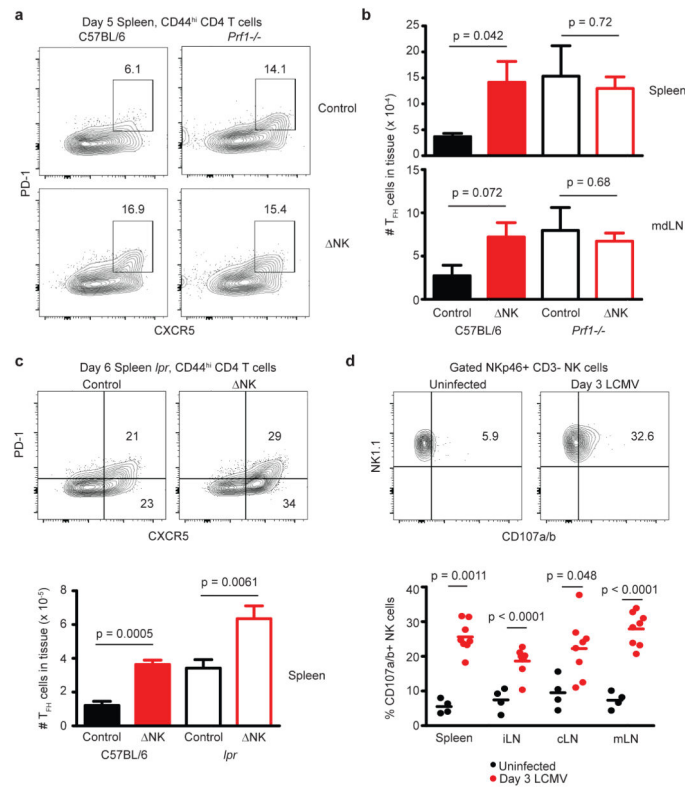


### Figure 9. NK cell suppression of T<sub>FH</sub> responses depends upon perforin

(a–c) Groups of C57BL/6, *prf1*<sup>-/-</sup>, or *lpr* mice (n = 8 per group) were depleted of NK cells (ΔNK) or administered control antibody (Control) one day prior to infection with LCMV Armstrong ( $5 \times 10^4$  p.f.u.). (a) Representative staining of T<sub>FH</sub> markers CXCR5 and PD-1 on activated (CD44<sup>hi</sup>) CD4 T cells in the spleen 5 days p.i. (b) Numbers of T<sub>FH</sub> cells (PD-1<sup>+</sup>CXCR5<sup>+</sup>CD44<sup>hi</sup>CD4<sup>+</sup>) in the spleen and mdLN at day 5 p.i. (± s.e.m.). (c) Proportion and number of T<sub>FH</sub> cells (± s.e.m.) in the spleen at day 6 of infection of C57BL/6 and *lpr* mice. (d) *Ex vivo* degranulation measured by CD107a/b staining of NKp46<sup>+</sup>CD3<sup>-</sup> NK cells in the spleen and LNs of uninfected or LCMV-infected (day 3 p.i.), and total number of degranulating (CD107a/b<sup>+</sup>) NK cells (n = 8 per group) is plotted. Results are pooled from two independent replicate experiments, and statistically significant differences were determined using Student's *t*-test.